Electronic Supplementary Information (ESI)

Template-free synthesis of nitrogen doped carbon materials from an organic ionic dye (Murexide) for supercapacitor application

Monazza Serwar[a,b], Usman Ali Rana[c*], Humaira M. Siddiqi[a*], Salah Ud-Din Khan[c], Fekri A. Ahmed Ali[d], Ahmed Al-Fatesh[d], Arturas Adomkevicius[b], Jose A. Coca-Clemente[b], Laura Cabo-Fernandez[b], Filipe Braga[b], Laurence J. Hardwick[b]

*[a]*Department of Chemistry, Quaid-I-Azam University Islamabad, Pakistan. Email: humairas@qau.edu.pk*

[b]*Stephenson Institute for Renewable Energy, Department of Chemistry, University of Liverpool, L69 7ZF, United Kingdom*

*[c]*Sustainable Energy Technologies (SET) centre, college of engineering, PO−Box 800, King Saud University, Riyadh 11421, Saudi Arabia. Email: urana@ksu.edu.sa*

[d]*Chemical Engineering Department, college of engineering, PO−Box 800, King Saud University, Riyadh 11421, Saudi Arabia.*

Contents

Table S1: Elemental composition of $NCM_{(MDE)}$-X by CHN microanalysis

Sample ID	C	H	N
$NCM_{(MDE)}$-700	61.64	1.78	19.51
$NCM_{(MDE)}$-800	61.29	1.62	13.75
$NCM_{(MDE)}$-900	63.34	1.37	7.17

Thermal studies

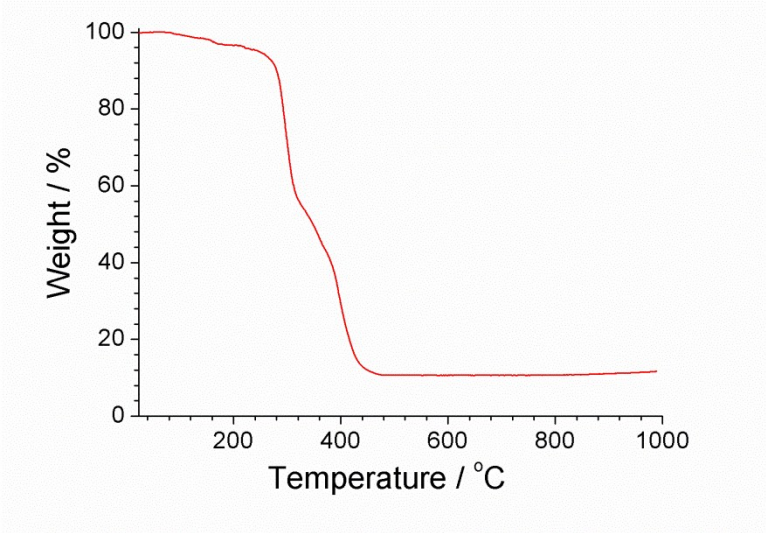

Figure S1: TGA of murexide under N_2 flow.

Morphology characterization

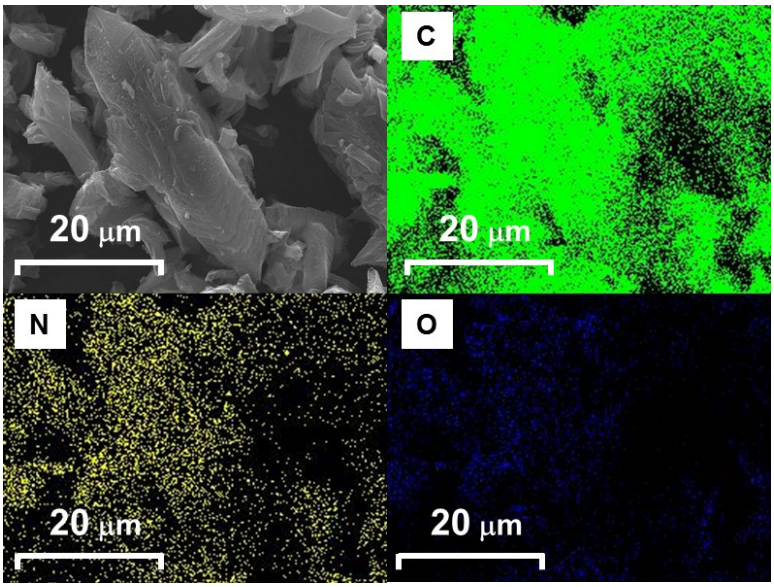

Figure S2: SEM image and EDS elemental maps of NCM $_{(MDE)}$-800.

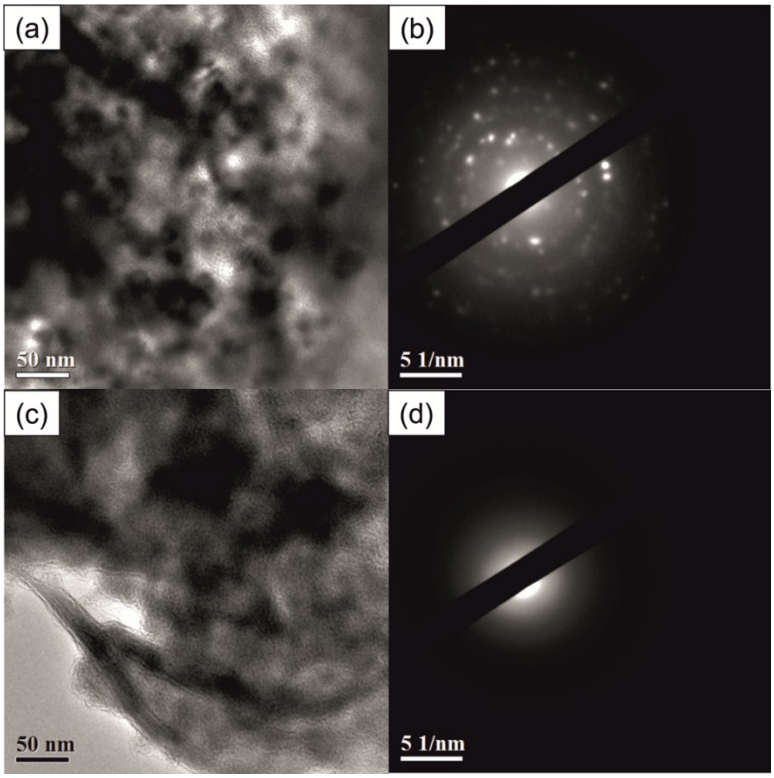

Figure S3: TEM images for NCM $_{(MDE)}$-800 and their corresponding SAED pattern in two different areas of the sample. Figure **(b)** shows the diffraction from the lattice in the crystalline part and **(d)** diffuse rings from the amorphous area.

BET Isotherms

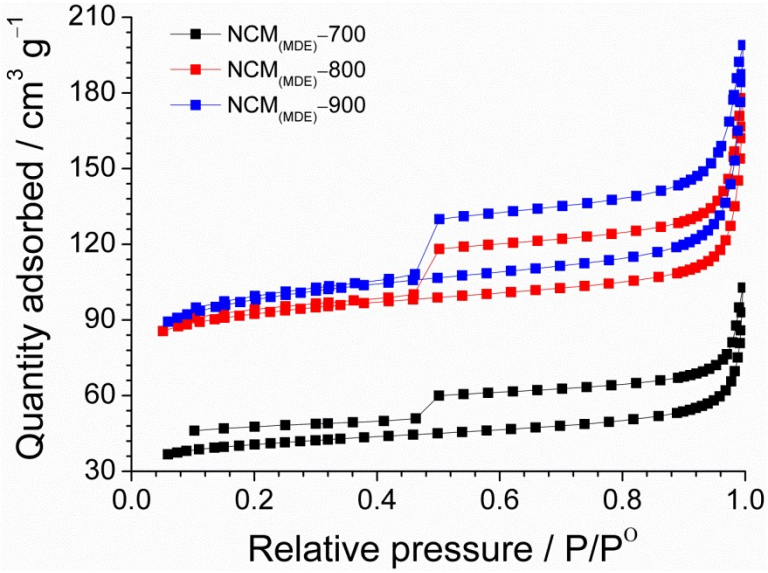

Figure S4: N_2 adsorption desorption Isotherms for NCM $_{(MDE)}$-X samples via Brunauer-Emmett-Teller (BET) characterization.

PSD curves

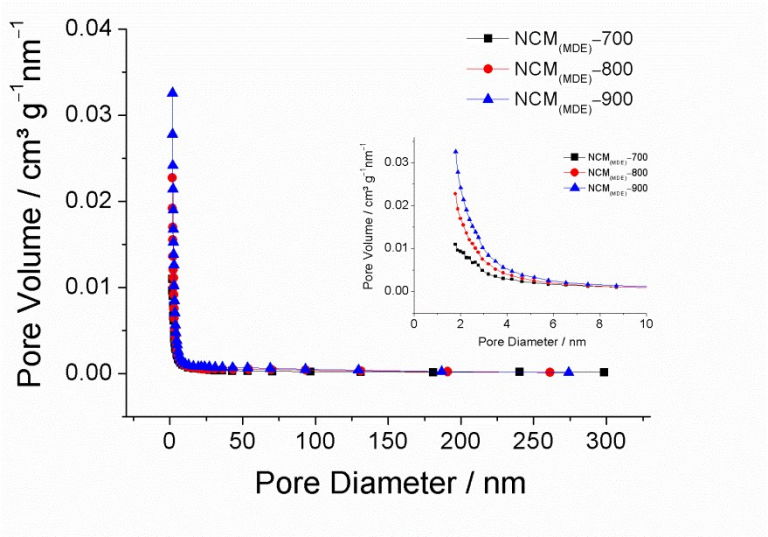

Figure S5: PSD curves for NCM $_{(MDE)}$-700, NCM $_{(MDE)}$-800 and NCM $_{(MDE)}$-900. The inset displays the pore size distribution data for these materials up to 10 nm.

Table S2: BET analysis data for NCM $_{(MDE)}$-700, NCM $_{(MDE)}$-800 and NCM $_{(MDE)}$-900.

BET Parameter	**NCM$_{(MDE)}$-700**	**NCM$_{(MDE)}$-800**	**NCM$_{(MDE)}$-900**
Surface Area ($m^2\ g^{-1}$)	127.88	286.51	306.68
Average pore diameter (nm)	11.46	10.09	9.39
t-plot micropore volume ($cm^3\ g^{-1}$)	0.042	0.11	0.11
Total pore volume ($cm^3\ g^{-1}$)	0.094	0.13	0.16
Average particle size (nm)	46.92	20.94	19.56

Electrochemical Studies

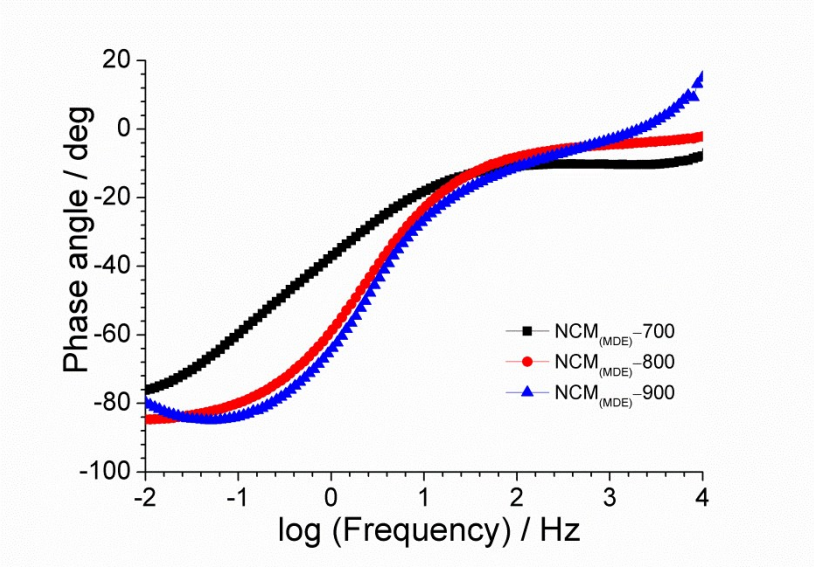

Figure S6: Bode plots for NCM$_{(MDE)}$-700, NCM$_{(MDE)}$-800 and NCM$_{(MDE)}$-900 electrodes

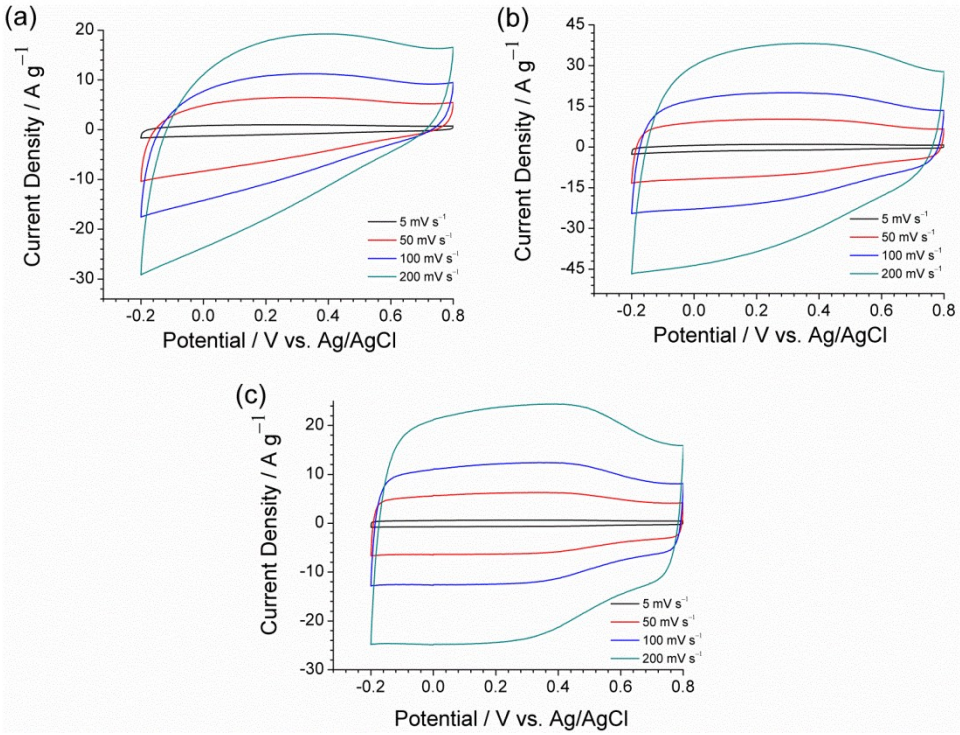

Figure S7: Cyclic voltammograms of **(a)** $NCM_{(MDE)}$-700, **(b)** $NCM_{(MDE)}$-800, and **(c)** $NCM_{(MDE)}$-900 at different scan rates in 1.0 M H_2SO_4.

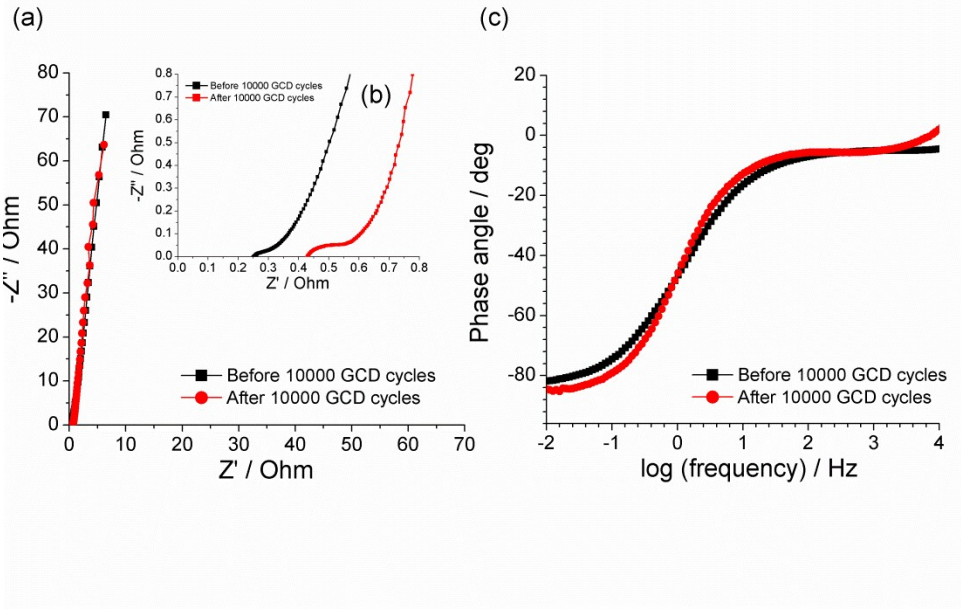

Figure S8: Electrochemical impedance spectra; **(a)** Nyquist plot, **(b)** Nyquist plot: magnified region 0-0.8Ω) and **(c)** Bode plot of $NDM_{(MDE)}$-800 electrode show the effect of long CD cycling upto 10,000cycles at 10A g^{-1}.

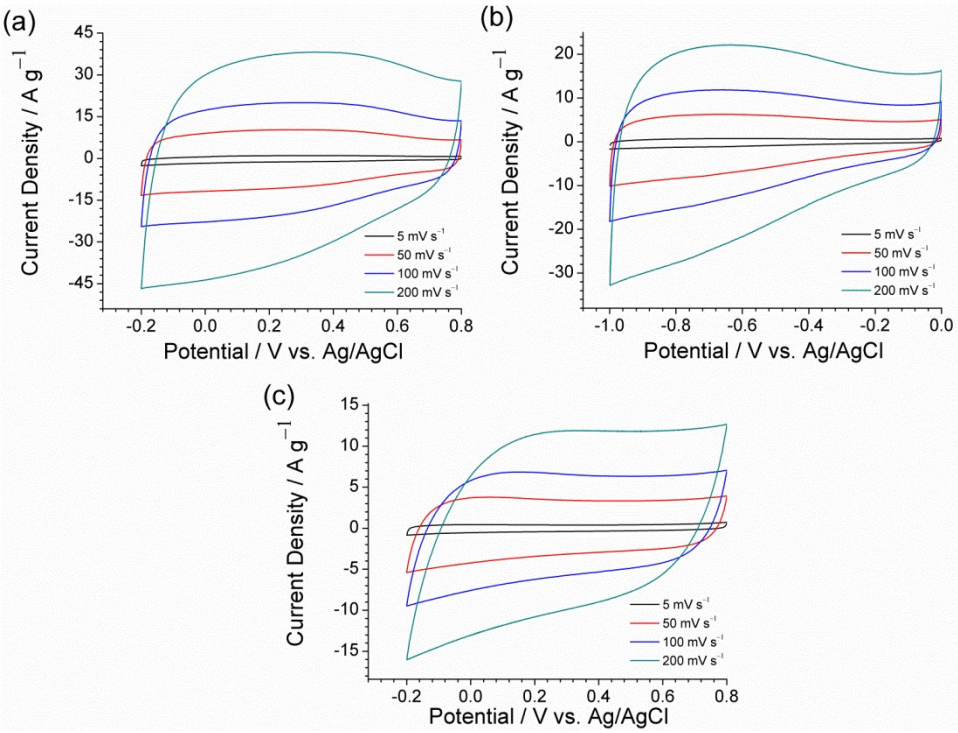

Figure S9: Cyclic voltammograms of NCM $_{(MDE)}$-800 electrode at different scan rates in different electrolytes; **(a)** 1.0 M H_2SO_4, **(b)** 6.0 M KOH and **(c)** 0.5 M Na_2SO_4

No major shape changes are observed in the CV curves recorded in 1 M $H_2SO_{4(aq)}$ and 6 M $KOH_{(aq)}$with increasing scan rate, particularly at high scan rate of 200mV s^{-1} Figure S9. This indicates that $NCM_{(MDE)}$-800 has high rate capability in both acidic and basic electrolyte media. In contrast, the CV curves recorded in 0.5 M $Na_2SO_{4(aq)}$, clearly show a distortion in the shape as the scan rate increases, indicating a poor rate capability in this electrolyte system when compared with acid and basic media.